Midcrustal emplacement of the Sausfjellet pluton, central Norway: Ductile flow, stoping, and in situ assimilation

Gregory Dumond[†]
Aaron S. Yoshinobu[‡]
Calvin G. Barnes
Department of Geosciences, Texas Tech University, Lubbock, Texas 79409-1053, USA

ABSTRACT

Midcrustal (25–30 km) emplacement of the dioritic Sausfjellet pluton into rocks of the Helgeland Nappe Complex, central Norway, occurred in two stages. Stage 1 consists of two-pyroxene hornblende gabbro and diorite. Stage 2 is asymmetrically zoned, with a modally layered central zone of diorite and anorthosite and a western/annular zone of quartz-bearing monzodioritic rocks. Igneous layering was locally attenuated, folded, and boudinaged in the hyper-solidus state. The magmatic foliation trajectory pattern in the pluton defines a shallowly southwest-plunging synform that crosscuts compositional zones. Mineral lineations plunge shallowly to moderately to the southwest. The pluton intruded a major lithologic boundary within the nappe; migmatitic pelitic gneisses are the main host rocks to the western part of the pluton, whereas the eastern and central parts are hosted predominantly by metacarbonate rocks. Calc-silicate, marble, quartzo-feldspathic, and dioritic xenoliths (up to 200 m in length) are present throughout the pluton; they are most common in Stage 1 and the central zone of Stage 2. Metapelitic xenoliths are conspicuously absent. Ductile flow during emplacement produced an ~1-km-wide structural aureole in which host-rock structures were deflected into subparallelism with the steeply inward-dipping margin of the pluton. Tight antiforms developed along the northeastern, southeastern, and southwestern margins. Amphibolite-grade shear zones in the host rocks preserve pluton-side-up kinematic indicators. In addition to the abundance of dioritic, calc-silicate, and quartzo-feldspathic gneiss xenoliths and geochemical evidence for assimilation in the western/annular zone, regional discordance of the pluton–host-rock contacts indicates that stoping was also an important emplacement process at midcrustal depths. Following magma emplacement, foundering of the central portion of the chamber combined with possible ca. 445 Ma regional contraction produced the map-scale synform defined by magmatic foliations and igneous layers. This study demonstrates that stoping and assimilation may occur simultaneously with host-rock ductile flow during magma chamber evolution at midcrustal levels and offers an explanation of why xenolith preservation may be compositionally dependent.

Keywords: pluton emplacement, stoping, layered intrusions, Caledonides, Bindal Batholith.

INTRODUCTION

Since A.F. Buddington's 1959 seminal examination of North American pluton–host-rock systems, geologists have recognized the first-order depth dependence of various magma emplacement mechanisms. Many workers have documented the diversity of physical processes that attend magma emplacement with respect to depth and temperature (e.g., Buddington, 1959; Pitcher, 1979; Marsh, 1982; Paterson et al., 1996; McNulty et al., 2000), yet many published magma emplacement models attempt to identify a single prevailing mechanism for the construction of plutons (e.g., Holder, 1979; Hutton, 1988; Tikoff and Teyssier, 1992; Morgan et al., 1998; and others). In general, such models involve either brittle or ductile deformation in the form of faulting/shearing (e.g., Tikoff and Teyssier, 1992) or ductile flow (e.g., Holder, 1979). Most such studies have been carried out on shallow to middle crustal plutons; fewer focused on construction of magma chambers in the middle to deep crust (Paterson and Miller, 1998).

During magma ascent and emplacement, host rocks may not respond in either a strictly brittle (e.g., diking) or ductile (e.g., diapirism) manner (Rubin, 1993; Miller and Paterson, 1999). This is particularly true at middle to deep crustal levels, where diverse emplacement-related features suggest the operation of both brittle and ductile (i.e., viscoelastic) processes during magma chamber construction (Rubin, 1993).

Many structurally oriented emplacement models do not take into account the compositional evolution of the magma, which commonly evolves as an open system. For example, while assimilation and hybridization are well documented in arc magmas, it is less clear what physical processes initiate assimilation during the evolution of a magma. Magmatic stoping (Daly, 1903) is one mechanism that can incorporate crustal material into a magma chamber and initiate assimilation (e.g., Clarke et al., 1998). However, such processes are generally not considered in magma emplacement models. Since the efficacy of stoping is contentiously debated (compare Marsh, 1982; Clarke et al., 1998; Yoshinobu et al., 2003; with Clemens and Mawer, 1992; Petford, 1996; Tikoff et al., 1999), evidence for stoping and for its consequences on magmatic evolution will provide interesting constraints on the compositional evolution of magmas *and* the mechanisms of emplacement.

Here we report on the emplacement and structural evolution of the Sausfjellet pluton, a laterally zoned dioritic body in the Norwegian Caledonides (Fig. 1A and 1B). The pluton was emplaced at middle crustal depths by a combination of stoping and ductile flow of its host rocks. Geologic and geochemical evidence presented in Barnes et al. (2004) indicates that lateral zoning developed, at least in part, because of differences in compositions of the

[†]Present address: Department of Geosciences, University of Massachusetts, 233 Morrill Science Center, Amherst, Massachusetts 01003-9297, USA.
[‡]Corresponding author e-mail: aaron.yoshinobu@ttu.edu.

GSA Bulletin; March/April 2005; v. 117; no. 3/4; p. 383–395; doi: 10.1130/B25464.1; 9 figures; 1 table.

host rocks, such that the parts of the pluton hosted by metacarbonates show little chemical evidence of host-rock contamination, whereas parts hosted by metapelitic migmatites show chemical and isotopic evidence for stoping and assimilation. In this report we first present the geologic setting of the pluton and document emplacement-related deformation of the host rocks. This is followed by a description of the structural features of the pluton and then by a model for magma emplacement.

GEOLOGIC SETTING

The Sausfjellet pluton intrudes the Helgeland Nappe Complex, which is the uppermost nappe complex in the Caledonides of north-central Norway (Fig. 1A and 1B). In the Velfjord region, the Helgeland Nappe Complex has been divided into four nappes; from structurally lowest, they are the Soren-Torghatten, lower, middle, and upper nappes (Fig. 1B; Thorsnes and Løseth, 1991; Yoshinobu et al., 2002). The Soren-Torghatten and middle nappes consist of basal ophiolitic rocks that are unconformably overlain by medium-grade metasedimentary sequences. The lower and upper nappes consist of migmatitic paragneiss, marble, calc-silicate rocks, and sparse amphibolite. The nappes are separated by east-dipping shear zones. Displacement on these shear zones was originally in a west-vergent reverse sense; however, the shear zones between the Sauren-Torghatten and the lower nappes, and between the lower and the middle nappes show down-to-the-east, normal displacement reactivation (Yoshinobu et al., 2002). The timing and nature of the regional deformation during the interval when the Sausfjellet pluton was constructed is summarized in Table 1.

During an arc collisional event, migmatization of pelitic and quartzo-feldspathic rocks of the lower nappe accompanied upper amphibolite facies regional metamorphism and emplacement of a number of peraluminous plutons. The regional metamorphic event occurred from 477 to 468 Ma (Barnes et al., 2002; Yoshinobu et al., 2002) based on U-Pb (zircon) ages of synmetamorphic granites. Between 448 and 430 Ma (Nordgulen et al., 1993; Yoshinobu et al. 2002), the compositionally diverse Bindal Batholith was emplaced. In the Velfjord region, the batholith consists of the predominantly dioritic Velfjord plutons (Fig. 1B; Akset-Drevli, 447.8 ± 2.3 Ma; Hillstadfjellet, 447.0 ± 3.2 Ma; and Sausfjellet, 445 ± 11 Ma; Yoshinobu et al., 2002) and the 447 ± 7 Ma Andalshatten pluton (Nordgulen et al., 1993). Emplacement pressures for these four plutons were in the 600–800 MPa range (20–30 km) based on garnet-aluminosilicate-quartz-plagioclase and aluminum-in-hornblende barometry on samples with the appropriate mineral assemblage (Barnes and Prestvik, 2000).

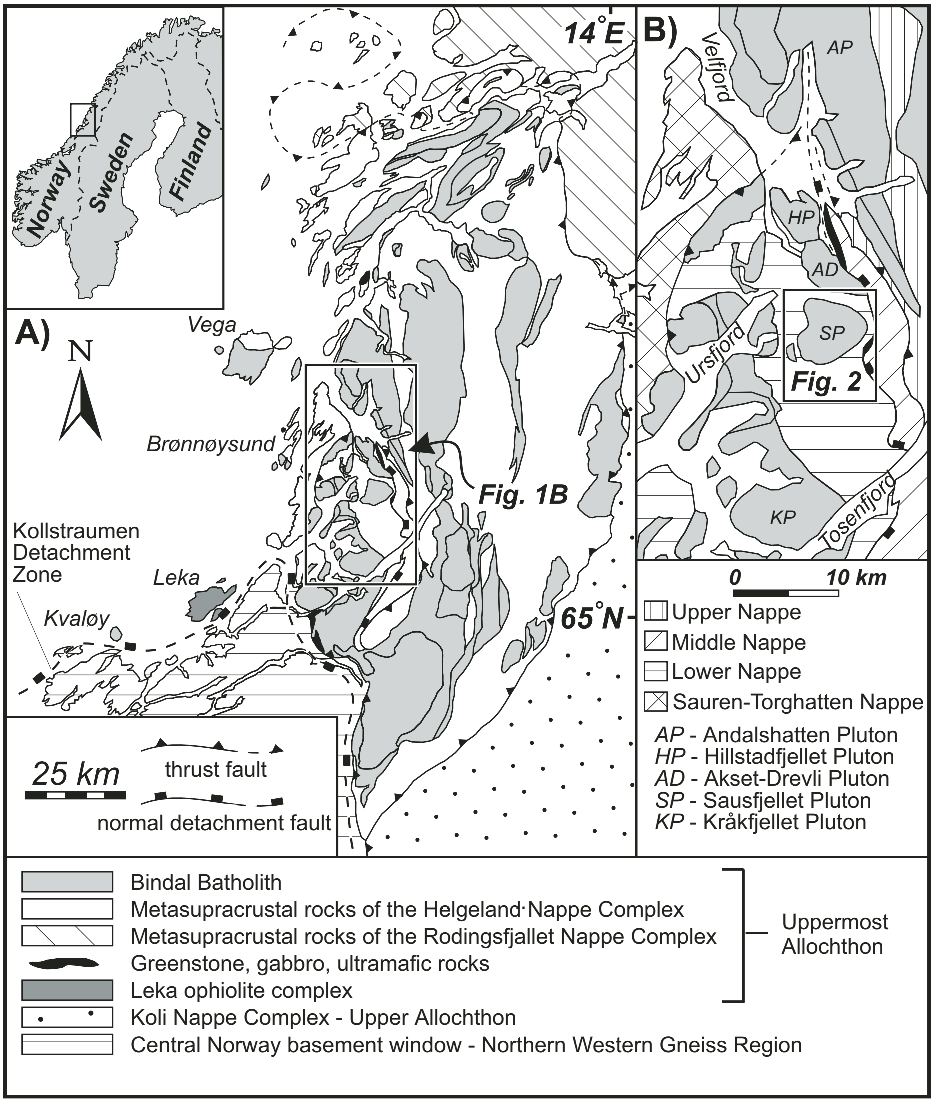

Figure 1. (A) Location map modified after Nordgulen and Sundvoll (1992) illustrating the geologic setting of the Helgeland Nappe Complex, Scandinavian Caledonides. (B) Inset depicts major shear zones in the Helgeland Nappe Complex and the localities discussed in the text.

GEOLOGY OF THE SAUSFJELLET PLUTON AND AUREOLE

Host Rocks

The western side of the pluton is hosted primarily by migmatitic pelitic gneiss with minor marble and amphibolite; the eastern half is hosted by marble, calc-silicate rocks, and minor migmatitic pelitic gneiss (Fig. 2). The contact aureole is ~1 km wide and is defined by the deflection of foliations and lithologic contacts into steeply dipping orientations subparallel to the intrusive contacts (Fig. 3) and on the west by disruption of layering in regional migmatite to form diatexite (disrupted migmatite; e.g., Barnes et al., 2002). The aureole's southern extent is inferred from the deflection of foliation trajectories and the change in dip direction of lithologic units (Fig. 3). As described below, discontinuously developed shear zones in the inner aureole of the pluton are generally defined by pluton-side-up kinematics.

The western contact with the migmatitic gneiss is locally defined by an ~100–200-m-wide zone of interfingering, contact-parallel dikes of diorite, diatexite, and two-mica granite (Fig. 2; Barnes et al., 2002). As this contact is

TABLE 1. SUMMARY OF REGIONAL STRUCTURAL/METAMORPHIC EVOLUTION OF ROCKS WITHIN THE LOWER NAPPE OF THE HELGELAND NAPPE COMPLEX, CENTRAL NORWAY.

Structural event	Age (Ma)	Reference
West-directed contraction and associated folding, migmatization, and granite petrogenesis associated with arc collision	477–466	Yoshinobu et al. (2002); Barnes et al. (2002)
West-directed contraction associated with "Taconic"-like arc-continent collision	468–448	Yoshinobu et al. (2002)
Emplacement of Velfjord plutons, development of the Sausvatnet shear zone within the aureole of the Sausfjellt pluton, and local north-south contraction associated with exhumation of lower nappe along the Skogmoen detachment fault	ca. 447–445	Barnes and Prestvik (2000, 2002); Dumond (2002); Yoshinobu et al. (2002)

approached, fold axes in the migmatitic gneiss change orientation from moderate SE–plunging to shallowly SSE plunging. Sillimanite lineations plunge moderately to the SE (Fig. 2).

With approach to the northern contact, calc-silicate layers in marble are ptygmatically folded and locally boudinaged. Moderately to steeply plunging mullions occur at the contact between the marble and the diorite. Apophyses of diorite inject coarsely recrystallized marble and locally contain xenoliths of the marble. Sillimanite lineations in migmatitic gneiss near the contact plunge shallowly to moderately to the southeast and northwest, whereas in the pluton, lath-shaped hornblende lineations plunge steeply to the southeast (Fig. 2).

Along the northeastern and southeastern margins of the pluton, the migmatitic gneiss pinches and swells along strike and becomes laterally discontinuous (Figs. 2 and 3). In these areas and along the southwestern margin, shallowly to moderately plunging tight antiformal folds defined by metamorphic layering in the marble and gneiss are present (Figs. 3 and 4). These structures form discontinuous shear zones within the inner aureole of the pluton.

Along the northern side of the pluton, an ~1-km-wide shear zone strikes west-northwest, subparallel to the steeply southwest-dipping intrusive contact (Figs. 3 and 4A). The shear zone is bounded on its northern side by the Akset-Drevli pluton, whose margin dips moderately northward (Fig. 4A). This shear zone is termed the "Sausvatnet shear zone" after the lake that parallels its length (Fig. 3). Adjacent to the northeastern contact of the Sausfjellet pluton, leucosomes in migmatitic pelitic gneiss within the Sausvatnet shear zone are parallel to foliation and also occur in shear bands that cut across foliation. At a distance greater than ~1.2 km from the pluton, leucosomes are no longer apparent in the gneiss (near the bend in cross-section A–A′; Fig. 4A).

Foliations in the shear zone generally dip steeply to the southwest (Fig. 4A). Lineations defined by sillimanite in migmatitic pelitic gneiss and by graphite and mullions in the layered calc-silicate rocks and marble plunge shallowly to moderately to the southeast (Fig. 4A). Synkinematic sillimanite porphyroblasts along the northeastern side of Sausvatnet display top-to-the-northwest reverse displacement (i.e., pluton-side-up) (Fig. 5A). Crudely asymmetric garnet porphyroblasts with tails of sillimanite show a similar sense of displacement in migmatitic gneiss adjacent to the pluton (Fig. 5B). Calc-silicate layers in the marble are deformed into sigma-clasts and asymmetric boudins that also show dextral top-to-the-northwest reverse displacement on surfaces viewed perpendicular to the foliation and subparallel to the lineation. Along the western part of the shear zone, lineations in the migmatitic gneiss locally plunge shallowly to the southwest (Fig. 2). Kinematics of this part of the shear zone inferred from dynamically recrystallized asymmetric K-feldspar porphyroclasts yield dextral down-to-the-southwest normal-sense displacement.

As the eastern contact of the intrusion is approached, calc-silicate layers are ptygmatically folded, sheared, and boudinaged. Leucosomes in migmatitic gneiss locally intrude along the contact between the marble and the gneiss. Calc-silicate xenoliths (0.5–5 m in length) and mafic enclaves in the pluton have long axes subparallel to magmatic foliation and the host-rock foliation, both of which dip steeply to the southwest (Fig. 2). Lineations defined by prismatic hornblende are subhorizontal.

Along the southern margin, lineations in the migmatitic gneiss, calcareous schists, and quartzo-feldspathic gneiss plunge shallowly to moderately to the northeast and southwest (Fig. 2). A map-scale, sinistral deflection of foliation trajectories was mapped southwest of Strauman (Fig. 3). This is consistent with sinistral top-to-the-southwest normal displacement observed in sigma-type garnet porphyroblasts in the migmatitic gneiss along the southeastern margin, and sinistral, asymmetric folds (Fig. 4C) and top-to-the-southwest reverse displacement defined by C′-shear bands in folded calcareous schists and adjacent to the southwestern margin of the pluton (Fig. 5C). Together these observations indicate pluton-side-up displacement along the structures near the southern contact.

Along the southwestern margin a deformed monzodioritic dike that intruded marble and calcareous schists is subparallel to the steeply NE-dipping contact of the pluton. The dike is axial-planar to a shallowly SE-plunging z-fold that displays pluton-side-up sense of displacement.

In summary, lithologic contacts and foliations are conformable with the inward dip of the intrusive contact (Fig. 2). Shallow to moderately plunging lineations and asymmetric folds in the gneiss and calcareous schists in the contact aureole are consistent with a component of lateral expansion of the magma chamber into the host rocks. However, at the map scale the pluton is discordant; host-rock markers cannot be restored to their pre-emplacement configuration by "removing" the pluton from the map plane (Fig. 2; see also Discussion). The pluton cuts across an extensive body of migmatitic pelitic gneiss along the southwestern contact, even though foliation trajectories and fold axial surfaces are brought into subparallelism with the contact (e.g., Fig. 4).

Sausfjellet Pluton

The Sausfjellet pluton is asymmetrically zoned and was emplaced in distinct stages. The first stage underlies the southeastern part of the pluton. It consists of biotite-bearing two-pyroxene (clinopyroxene > orthopyroxene) hornblende gabbro and diorite (Fig. 6). Stage 1 can be distinguished in the field by its rusty orange weathering and the presence of dark brown hornblende oikocrysts up to 3 cm in diameter. A poorly exposed, sharp intrusive contact separates rocks of stage 1 from those of stage 2.

A small mass of gabbroic rock crops out southwest of the Sausfjellet pluton. The two bodies are separated by a septum of marble and pelitic migmatite (Fig. 2). This small gabbroic body, herein named the Nonsdalen pluton, consists of coarse- to medium-grained hornblende pyroxene gabbro and diorite. The unit is texturally similar to stage 1, but poor exposure and extensive deuteric alteration limited our collection and description to a few samples.

Stage 2 is asymmetrically zoned from east to west (Fig. 6) and is subdivided into central and western/annular zones on the basis of internal structure, mineral assemblages, and geochemical characteristics, as described below. The *central zone* is predominantly biotite two-pyroxene diorite (Fig. 6). Orthopyroxene is more abundant than clinopyroxene, and hornblende is an

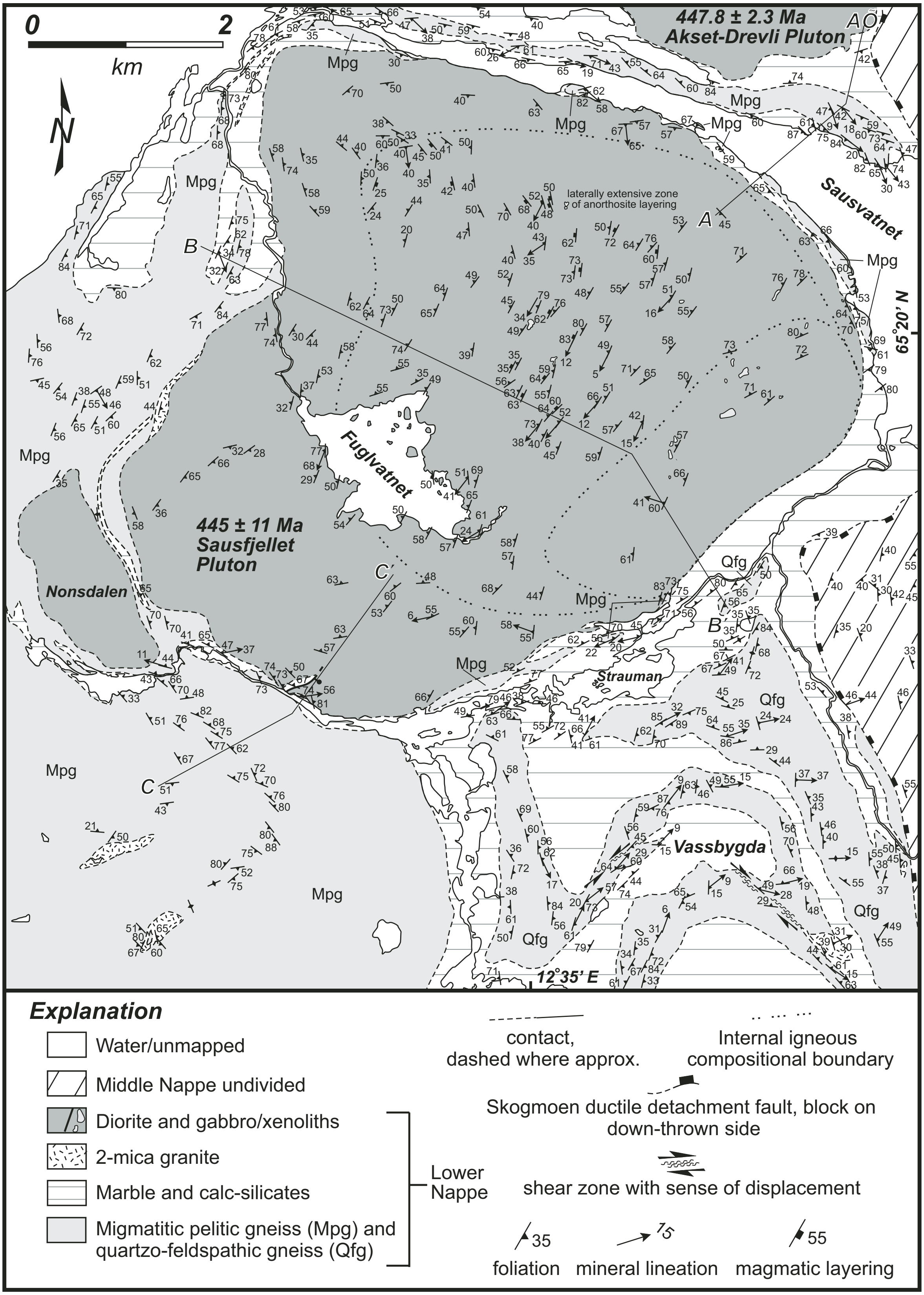

Figure 2. Geologic map of the Sausfjellet region, Velfjord, Norway. The map includes previously published data from Kollung and Myrland (1970), Skaarup et al. (1974), Thorsnes (1985), and Barnes et al. (1992). Unpublished data collected between 1987 and 1988 in the northwest quadrant of the map by M. Schöenfeld and colleagues from Technische Universität Clausthal, Germany, have also been included. Lines of cross sections (A–A′, B–B′, and C–C′) in Figure 4 are indicated.

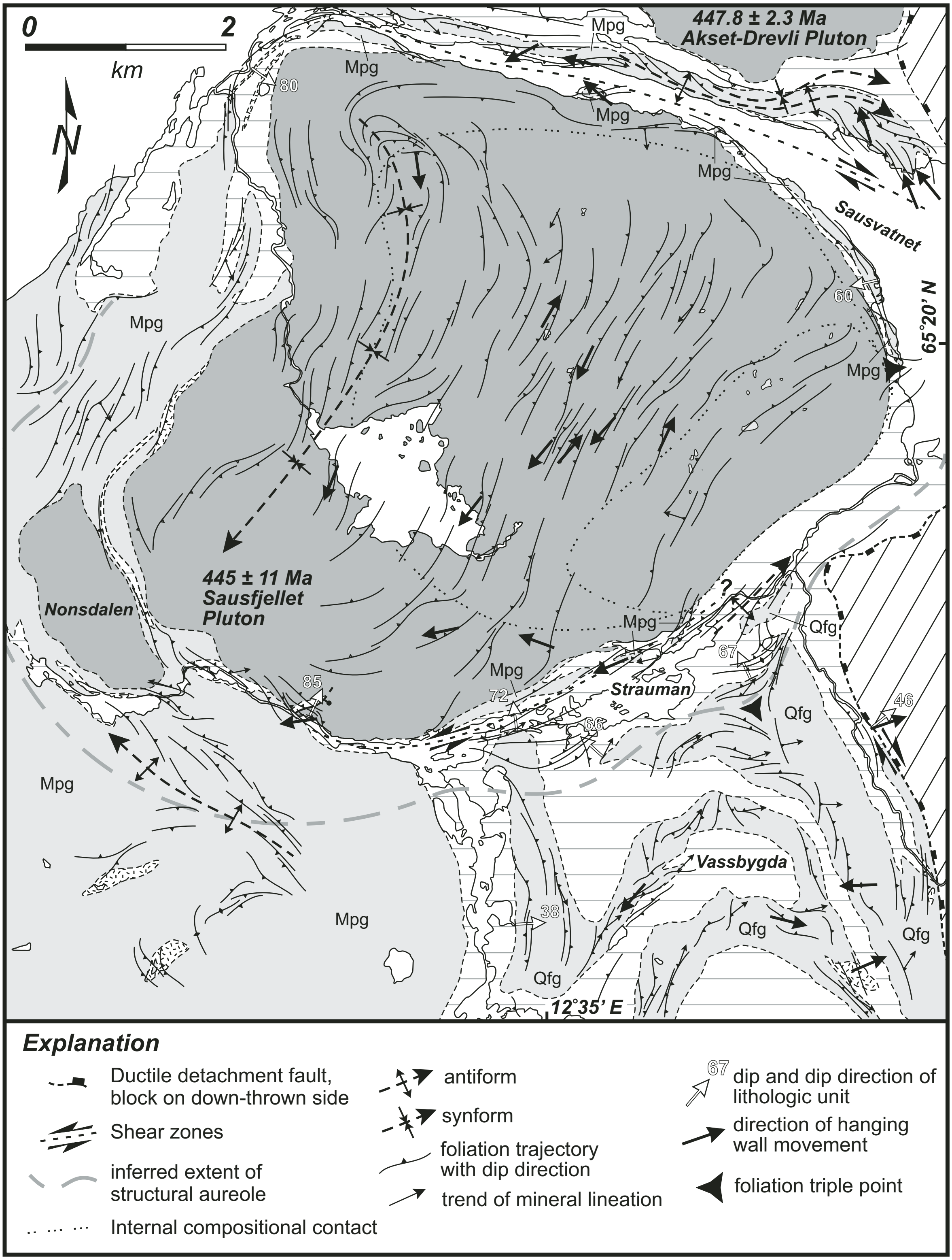

Figure 3. Foliation trajectory map based on data presented in Figure 2; lithologic legend same as in Figure 2.

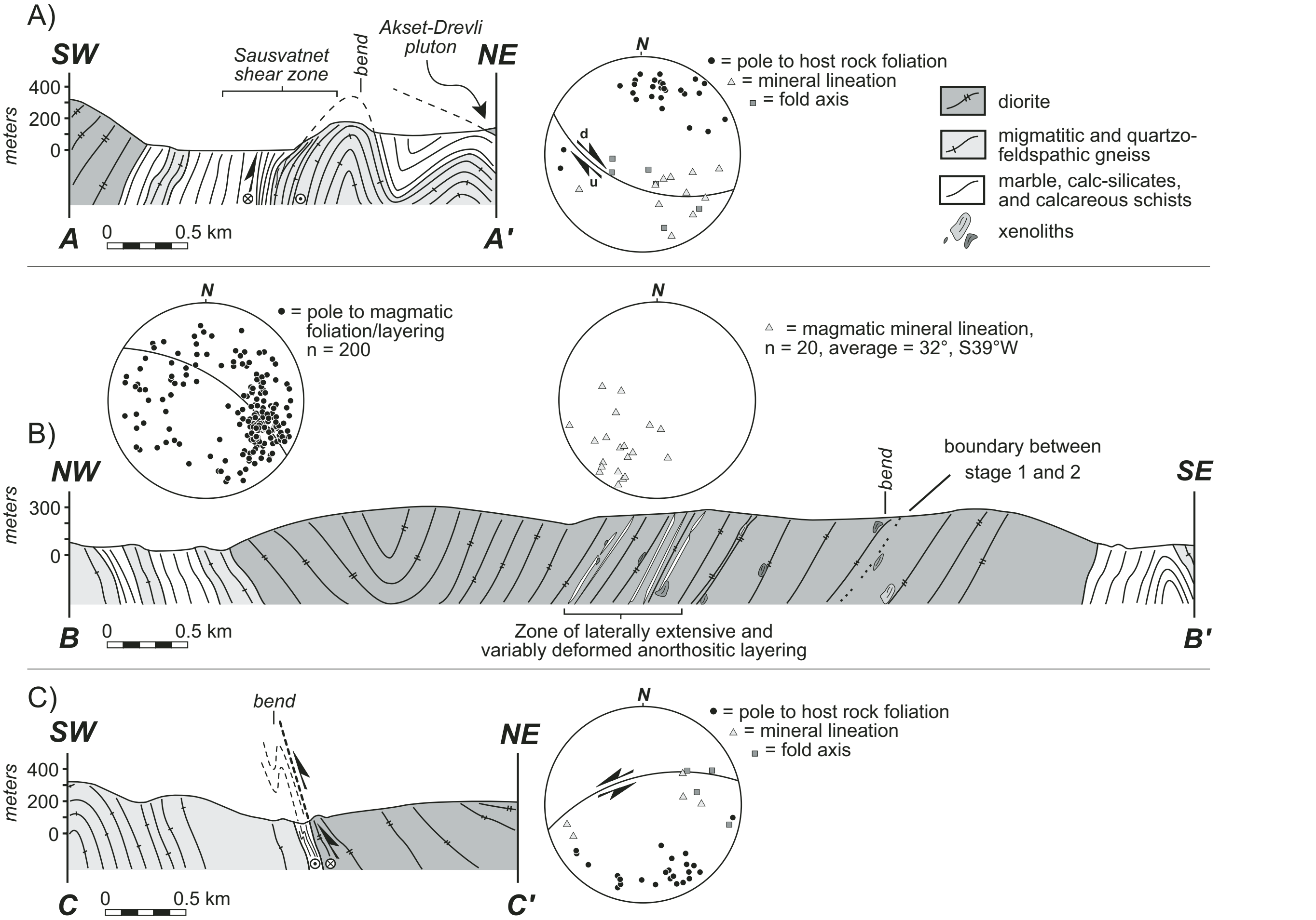

Figure 4. Interpretive cross sections of the Sausfjellet pluton and aureole with lower hemisphere equal-area projection stereonet data. (A) Dextral top-to-the-northwest reverse Sausvatnet shear zone and projection of moderately north-dipping contact of Akset-Drevli pluton. (B) Magmatic foliation/layering and lineations within the pluton. (C) Sinistral shear zone along the southern and southwest margin of the pluton displaying pluton-up kinematics. Position of cross sections through pluton indicated in Figure 2.

accessory phase. Centimeter- to decimeter-thick anorthosite and pyroxene-rich diorite layers (<1 to >300 m long) crop out in the northern part of the central zone (Fig. 7A–7C). Contacts between anorthosite layers and the more abundant two-pyroxene diorite layers are sharp and locally lobate. Some diorite layers are modally graded, with pyroxene-rich and less commonly magnetite-rich basal zones that grade upward into plagioclase-rich rock (Fig. 7B). Layering is discontinuous along strike, may be folded (e.g., Fig. 7B), and commonly displays pinch and swell structures and tapered ends (Fig. 7C). Synmagmatic normal-sense shear bands that displace layers down to the southwest are locally common (Fig. 7D). Schlieren are present throughout the central zone and consist of diffuse segregations of mafic minerals.

Dioritic rocks of the central zone grade westward and outward to a zone of more variable lithology. This transition is defined on the basis of petrographic features, the absence of layering, a decrease in the intensity of foliation, and geochemical compositions (Barnes et al., 2004) and occurs over widths of tens to perhaps 100 m. We refer to these petrographically diverse rocks that underlie the western part of the pluton, as well as a nearly continuous annular ring around stage 1 and the central zone of stage 2, as the western/annular zone. The annular zone varies in width from 100 m to 1 km and contains numerous dikelike bodies of variable grain size and rock type, whereas the western zone is generally massive (Fig. 6).

Rock types in the western/annular zone are diorite, quartz diorite, monzodiorite, and quartz monzodiorite. As in the central zone, the proportion of low-Ca pyroxene is greater than augite. However, hydrous mafic minerals are more abundant and inverted pigeonite is present in some samples (Barnes et al., 2004). Thus, the western/annular zone is distinguished by its greater modal abundances of quartz, biotite, K-feldspar, and hornblende, paucity of modal layering, and generally weaker foliation.

Foliation and Microstructures

Foliation is defined by pyroxene and laths of subhedral to euhedral plagioclase with strong shape-preferred and lattice-preferred orientations (Fig. 7D and 7E). Plagioclase contains deformation twins and undulose extinction but little evidence for pervasive dislocation creep. Microfractures in pyroxene are generally subperpendicular to foliation. Weakly to well-developed mineral lineations defined by plagioclase laths and elongate prismatic pyroxene plunge shallowly to moderately to the southwest (Figs. 3 and 4B). We interpret the foliation and lineation to be

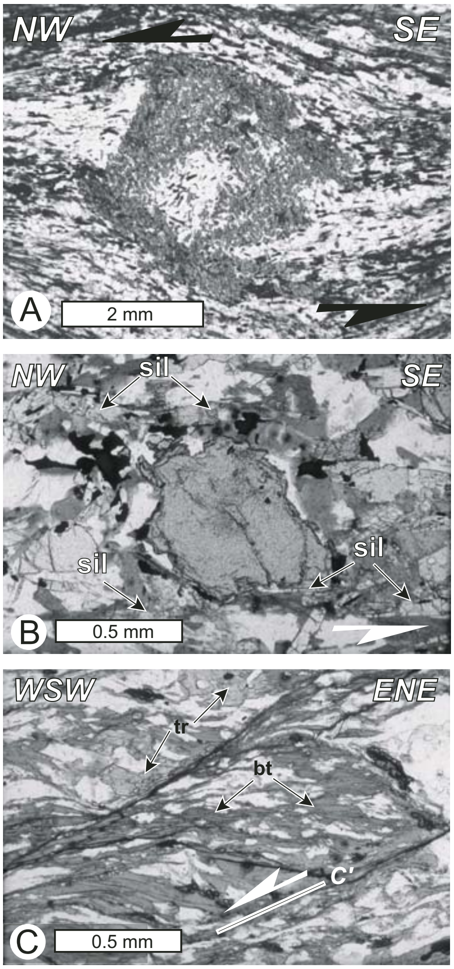

Figure 5. Kinematics in shear zones developed in the contact aureole of the Sausfjellet pluton. Photomicrographs are in plane light and are perpendicular to foliation and parallel to lineation. (A) Photomicrograph of synkinematic sillimanite porphyroblast from migmatitic pelitic gneiss, Sausvatnet shear zone, northern portion of aureole. (B) Asymmetric garnet porphyroblast with inclusions of fibrolite and tails of sillimanite (sil), Sausvatnet shear zone, northeastern portion of aureole. (C) C′ shear bands (extensional crenulation cleaveage) in calcareous tremolite (tr) + biotite (bt) schist in the limb of a fold along the southwest contact of the pluton. Kinematics inferred from outcrop fold asymmetry, shear bands, and C′ shear bands are consistent with pluton-side-up sense of displacement (top to WSW; see Fig. 4C).

of hypersolidus origin on the basis of the well-developed shape- and lattice-preferred orientation in plagioclase and on the lack of pervasive intercrystalline plastic deformation.

In the central zone of stage 2, the foliations are parallel to igneous layers and define a synform that plunges shallowly to the southwest (Figs. 3 and 7B). Within tens of meters of the host-rock contact, magmatic foliations are commonly subparallel to the contact. The foliation trajectory pattern cuts across the compositional zoning in the pluton. There is not a strong increase in magmatic fabric intensity approaching the host-rock contact.

Asymmetric fabrics, tiled plagioclase laths, and magmatic C-S fabrics are visible in thin sections cut perpendicular to the foliation and parallel to the mineral lineation (Fig. 7D). Shear sense indicators typically record top-to-the-southwest normal displacement, although shear sense inferred from tiled plagioclase laths from a few localities in the eastern half of the central zone show top-to-the-northeast reverse displacement (see Fig. 3).

Near the margins of the intrusion (i.e., in the annular zone), samples are commonly inequigranular with interlobate grain boundaries. Plagioclase displays deformation twins, undulose extinction, kink bands, and well-developed shape- and lattice-preferred orientation (Fig. 7E). Quartz displays undulose extinction and subgrain development (Fig. 7E). Some samples have polygonal arrangements of plagioclase and quartz with well-developed triple junctions, no apparent shape-preferred orientation in plagioclase, and weakly developed lattice-preferred orientation in both plagioclase and quartz. A few localized, discrete anastamosing plastic shear zones occur along the southern and northern margins of the pluton.

Xenoliths

Xenoliths range in outcrop area from <1 m^2 to >400 m^2; they consist of marble, calc-silicate rocks, quartzo-feldspathic gneiss, and diorite. The dioritic xenoliths are characterized by a trachytoid texture defined by cm-scale, elongate, tabular laths of plagioclase. This fabric is strikingly similar to the trachytoid texture of the Akset-Drevli pluton (Barnes et al., 1992). No xenoliths of the pelitic migmatite were observed.

Marble xenoliths generally crop out in the annular zone along the northern and eastern parts of the pluton, in some places less than 1 m from the pluton–host-rock contact (see Fig. 8A). In contrast, calc-silicate xenoliths are present throughout the pluton: they decrease in abundance from stage 1 to the central zone and then the western/annular zone of stage 2. They typically consist of diopside ± plagioclase ± quartz ± epidote. Such xenoliths are much richer in diopside than are the calc-silicate host rocks. Akset-Drevli–type dioritic xenoliths are most abundant in stage 1, but are also present in the central zone of stage 2 (Fig. 8B–8E).

Some quartzo-feldspathic and calc-silicate xenoliths are fractured along and across foliation planes. These fractures are typically filled with veins of fine-grained diorite (Fig. 8B). At some localities in the central zone, xenoliths were fragmented in situ by apophyses of the diorite.

Structural relationships between magmatic fabrics in the host pluton, xenolith geometry, and internal structures within the xenoliths are complex. The long axes of the xenoliths are typically aligned subparallel to the strike of magmatic foliation and modal layering (Fig. 8C), and metamorphic foliations within calc-silicate, marble, and quartzo-feldspathic xenoliths are predominantly subparallel to magmatic foliation in the host pluton. In contrast, the magmatic foliation of Akset-Drevli–type diorite xenoliths, if present, is more commonly discordant to magmatic foliation in the host pluton. Layering is common below and above the "stratigraphic" location of the xenoliths. In some localities, layering developed structurally above the blocks is tapered and boudinaged, indicating that the layers formed during or soon after xenolith entrainment and may have been "draped" on top of the xenolith (Fig. 8D). In other cases the magmatic foliation is deflected and truncated by the xenoliths (Fig. 8D). Beyond a few centimeters to meters from the xenoliths, magmatic foliations within the Sausfjellet pluton maintain their regional NNE trend (Fig. 8E). These observations indicate that the crystal mush had sufficient yield strength to trap the blocks yet still deform at hypersolidus conditions.

DISCUSSION

We summarize the following observations/interpretations that bear on the discussion of the emplacement and evolution of the Sausfjellet pluton in the middle crust. (1) Lithologic contacts and structures were deflected into subparallelism with the steeply inward-dipping contact of the pluton and shear zones developed within ~1 km of the contact. (2) Tight antiforms formed along the margins of the pluton; shear zones in host rocks close to the contact preserve pluton-side-up kinematics. (3) Dioritic, calc-silicate, and quartzo-feldspathic gneiss xenoliths are well preserved within the pluton, whereas pelitic migmatitic xenoliths are conspicuously absent. (4) The pluton is asymmetrically zoned, petrographically and geochemically, with the most evolved rocks in the western and annular zone (Barnes et al., 2004). The zoning is compatible with host rock and xenolith lithology. (5) A southwest-plunging synform defined by magmatic foliations and igneous layers cuts across compositional boundaries, zonation of the magma, and igneous layers. Foliation also postdates "capture" of some of

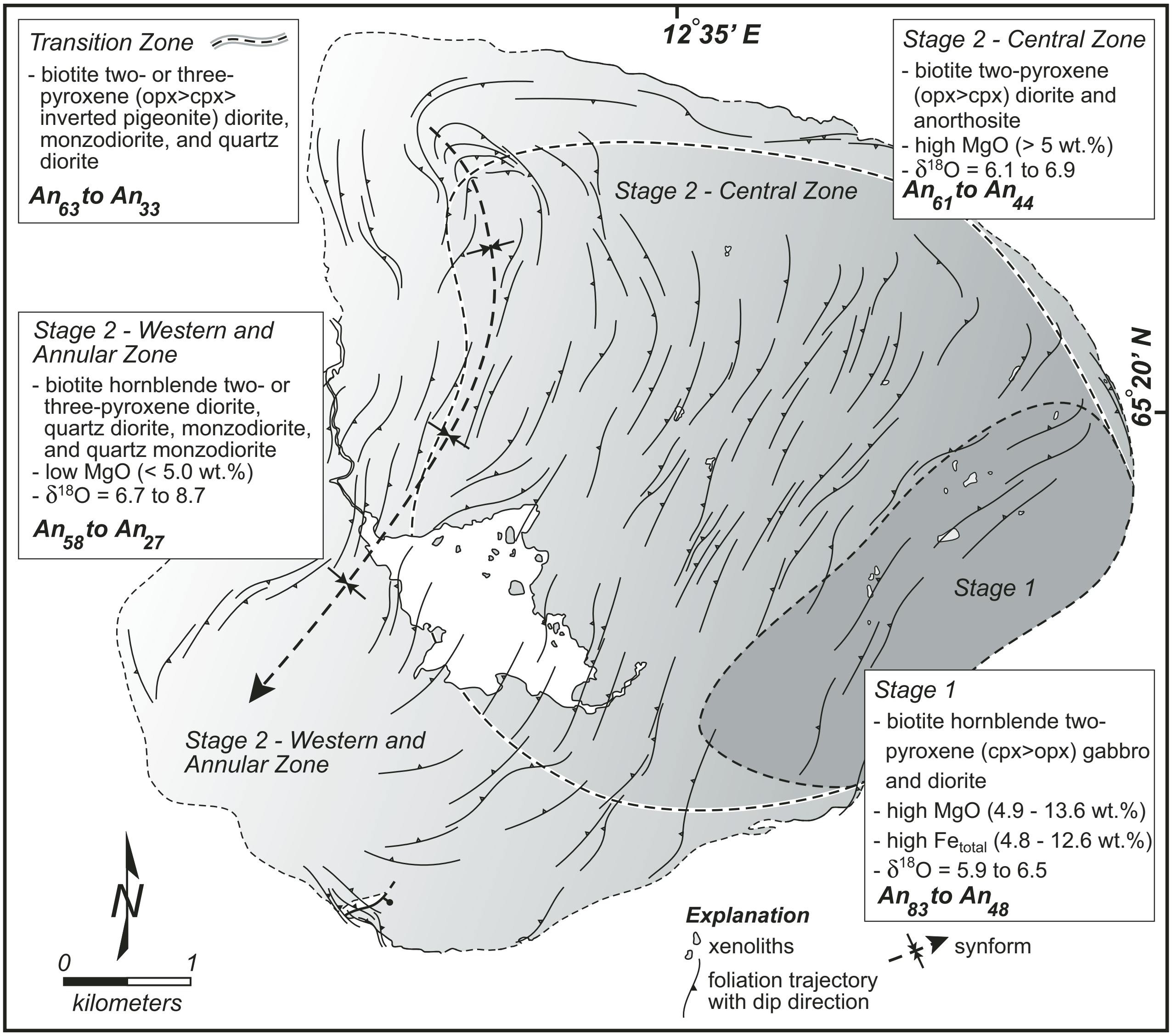

Figure 6. Map of lithologic, geochemical, and isotopic zoning in the Sausfjellet pluton. The contact between the central zone and western/annular zone is gradational. Note that foliation trajectories and synform axis cut across inferred compositional boundaries. Geochemical data from Barnes et al. (2004) and Dumond (2002).

the xenoliths because magmatic foliations wrap around most xenoliths.

Petrologic Evolution in the Context of Stoping and Emplacement

Three aspects of emplacement are noteworthy in the context of the petrological evolution of the Sausfjellet pluton (Barnes et al., 2004). First, the pluton was emplaced across a major lithologic boundary in the lower nappe that separates predominantly calcareous rocks in the east from pelitic migmatitic gneiss in the west. Second, magmatic stoping of the host rocks occurred, which produced regionally discordant contacts and resulted in the inclusion of a wide range of host-rock xenoliths within the pluton, but the absence of pelitic xenoliths. Third, contact metamorphism of pelitic host rocks resulted in remelting in the aureole, which produced diatexites (migmatites lacking continuous internal structures) adjacent to the pluton (Barnes et al., 2002). Contact migmatization occurred by biotite-dehydration melting in the temperature range of 800–850 ºC (Barnes and Prestvik, 2000). Based on mass balance calculations, Barnes et al. (2002) estimated that a minimum of 20%–25% melt was produced in the host pelitic migmatites during contact melting.

The intrusive contact between stage 1 and the central zone of stage 2 indicates that the Sausfjellet pluton is the product of at least two discrete pulses of magma (Fig. 6). The central zone of stage 2 behaved essentially as a closed system in which accumulation of variable proportions of plagioclase, clinopyroxene, and orthopyroxene resulted in the observed compositional trend. Barnes et al. (2004) suggested this process of in situ crystal accumulation also resulted in layer development and upward/inward aggradation of a cumulate pile of crystals. In the western/annular zone, however, the crude correlation of $\delta^{18}O$ values with differentiation, the increase in abundance of hydrous mafic phases, and an increase in incompatible trace elements beyond that predicted by closed-system fractionation suggests open-system behavior, specifically contamination by ^{18}O-, K_2O-, and Zr-rich

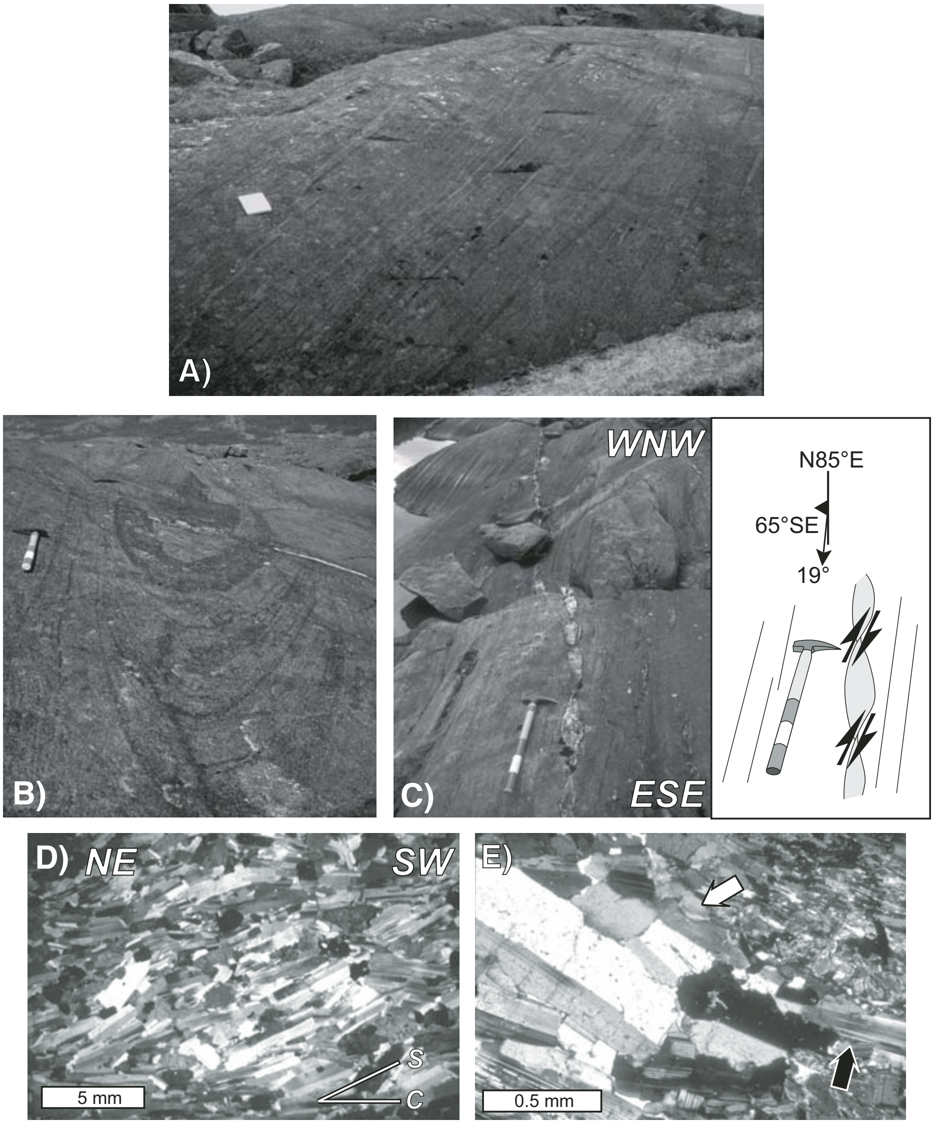

Figure 7. Field photos (A–C) and photomicrographs (D–E) of structures in the pluton. (A) View looking NNE at thin, well-developed anorthosite and diorite layers (notebook at left is 17 cm wide). (B) NNW view down-plunge of magmatic fold (head of hammer is 17 cm long). (C) Anorthosite boudins viewed NE along strike with accompanying sketch displaying dextral offset of boudins. (D) Dextral, down-to-SW magmatic C-S fabric in two-pyroxene diorite from central zone defined by tabular, elongate laths of plagioclase, view to the SE. (E) Magmatic foliation in quartz diorite from northern margin of pluton in the annular zone defined by the shape- and lattice-preferred orientation of plagioclase. Interstitial quartz contain subgrains (white arrow) and plagioclase contains some deformation twins (black arrow). Thin sections cut parallel to lineation, perpendicular to foliation.

material (Barnes et al., 2004). Their modeling is consistent with enrichment of hydrous phases and the increase in $\delta^{18}O$ due to a combination of crystal-liquid separation (i.e., fractionation) and assimilation of the migmatitic gneiss (Fig. 2). We suggest that assimilation resulted from stoping of blocks of already partly molten migmatitic gneiss into the stage 2 magma. As the blocks were incorporated into the stage 2 magma, their interstitial melts were extracted and mingled with the host magma, enriching it in ^{18}O, H_2O, and incompatible elements, specifically the alkalis (Barnes et al., 2004).

Stoping must have occurred throughout the emplacement history of the Sausfjellet pluton. This is supported by (1) the discordant contact between the migmatitic pelitic gneiss and the pluton along the southwestern margin (Fig. 2); (2) the presence of xenoliths along the margins of the intrusion, in stage 1, and in the central zone of stage 2 (Fig. 8); and (3) geochemical evidence for assimilation of pelitic migmatitic gneiss in the western/annular zone of stage 2 (Fig. 6; Dumond et al., 2002; Barnes et al., 2004). Although fracturing of a partially molten medium like the migmatitic gneiss in order to facilitate stoping at relatively high ambient temperatures requires rapidly applied strain (Rubin, 1993), dikes and apophyses from the pluton that intrude host rocks in the aureole suggest the presence of excess magma pressure, which may have contributed to this process.

Incorporation of pelitic migmatite via stoping is consistent with the observed compositional heterogeneity in the western/annular zone and with the regional geology. The Sausfjellet pluton intruded across a northwest- to northeast-striking regional contact between the pelitic migmatitic gneiss on the west and the marbles, calc-silicates, and quartzo-feldspathic rocks on the east (Fig. 2). This contact extends for ~45 km from the southern side of Velfjord to south of Tosenfjord (Gustavson, 1981). The gradational boundary between the closed-system part of stage 2 (the central zone) and the open-system part (western/annular zone) is essentially coincident with this regional contact. Stoping of marble, diorite, calc-silicates, and quartzo-feldspathic rocks into stage 1 and the central zone of stage 2 had little chemical effect on the magmas. In contrast, stoping of pelitic migmatite (with melt present) into the western/annular zone resulted in local, variable assimilation. Such variations probably reflect piecemeal stoping rather than uniform distribution of stoped blocks. The absence of such blocks is thought to be due to complete assimilation: The near-liquidus temperatures of the probable parental magma (ca. 1240 °C; Barnes and others, 2004) are high enough to accommodate dissolution of hot pelitic rocks (Patiño Douce and Johnston, 1991; Skjerlie et al., 1993). Furthermore, because the stoped blocks were partly molten, their porosity greatly increased the surface area in contact with the host, and they disintegrated quickly in the host diorite. Petrologic modeling presented in Barnes et al. (2004) is consistent with as much as 20% of the mass underlaying the western/annular zone to be derived from assimilated pelitic material.

Host-Rock Ductile Deformation

Ductile attenuation and transposition of the host rocks caused by outward expansion of the magma chamber would be possible at the high temperatures achieved during contact melting of the migmatites (800–850° C; Barnes and

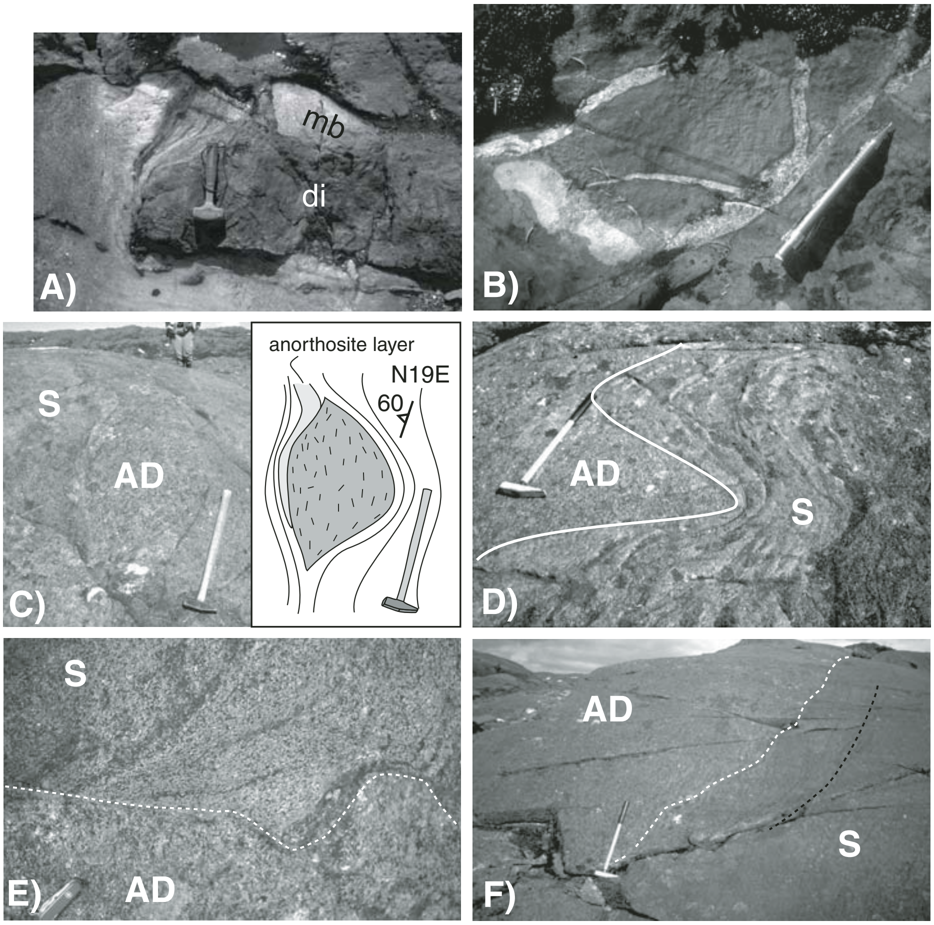

Figure 8. Field photographs of stoped blocks in the Sausfjellet pluton. (A) Apophysis of Sausfjellet diorite (di) at northern margin with included marble xenolith (mb). (B) Large xenolith of Akset-Drevli block surrounded by diorite of the Sausfjellet pluton. White dashed line denotes contact between xenolith and host; black dash represents magmatic foliation in the Sausfjellet pluton. (C) 1.5-m-long, deformed, lozenge-shaped Akset-Drevli–type xenolith (AD); accompanying field sketch illustrates the subparallel alignment of plagioclase laths in the xenolith with the foliation and deformed anorthosite layer; Sausfjellet pluton (S). (D) Close-up view of Akset-Drevli–type xenolith (AD) that deflects and truncates magmatic foliations and igneous layers in the Sausfjellet pluton (S). (E) Akset-Drevli–type diorite xenolith (AD) impinging on the aggraded floor of layered rocks in the Sausfjellet (S) pluton (hammer is 0.7 m long). (F) Fractured quartzofeldspathic xenolith intruded by fine-grained diorite (pencil is 13 cm long).

Prestvik, 2000; Barnes et al., 2002). Evidence for outward expansion of the magma chamber during emplacement includes the deflection of lithologic contacts and foliation trajectories in the surrounding host rocks, particularly near the southwestern and southeastern contacts of the intrusion (Figs. 3 and 4). Translation and ductile flow of the host rocks around the margins of the pluton would explain the presence of shallow to moderately plunging lineations and asymmetric folds in the gneiss and calcareous schists in the aureole.

Outward expansion of the pluton is also implied by the presence of tight plunging antiforms in the northeastern, southeastern, and southwestern parts of the aureole. The amount of strain that the folds accommodated during magma emplacement is dependent on the timing of folding. If the folds were already present and were tightened during emplacement, their presence signifies less expansion than if they formed during emplacement. Because the folds along the northeastern and southeastern margin of the pluton (Fig. 3) are oblique to the preexisting northwest-striking structural grain, their present geometry indicates significant transposition of the host-rock folds by emplacement-related strain (Dumond, 2002).

Finally, the discontinuous nature of the pelitic gneiss, particularly where it is concordant to the contact of the pluton, can be attributed to large-scale attenuation and boudinage. Outward expansion of the pluton and dextral oblique-slip to strike-slip shearing along the northern contact of the pluton can explain such deformation on the northern side of the pluton. Similar ductile flow would explain the translation of the migmatitic pelitic gneiss on the southern margin of the intrusion (northwest of Strauman in Fig. 2). Prior to emplacement, this gneiss was probably part of the large mass of pelitic gneiss southwest of the pluton.

A maximum amount of finite longitudinal strain produced by lateral expansion can be estimated from the map pattern of the southwestern part of the intrusion (Fig. 2). If one assumes that the northwest-striking contact between the pelitic gneiss (southwestern contact) and adjacent metamorphic rocks to the northeast was originally planar, then the amount of finite longitudinal strain produced by lateral expansion of the pluton into the pelitic migmatitic gneiss at the southwest portion of the intrusion was ~0.49 (as measured in map view). This estimate assumes plane strain and does not take into account the amount of volume lost due to stoping.

Emplacement as a Steep-Walled Intrusion or a Subhorizontal Tabular Body?

Numerous authors have suggested that subelliptical plutons can be characterized in three dimensions as tabular or funnel-shaped intrusions with floors that steepen toward one or more conduits (Vigneresse, 1995; Cruden, 1998; Wiebe and Collins, 1998). Floors that steepen toward a feeder are characteristic of a number of layered igneous intrusions (e.g., Muskox: Irvine, 1980; Skaergaard: McBirney, 1996). Models for the development of subhorizontal tabular plutons typically involve: (1) horizontal fracture propagation and/or magma accumulation at some anisotropic level in the crust (e.g., Hogan and Gilbert, 1995), (2) lateral growth or ballooning, and (3) floor subsidence accommodated by either normal-sense movement on basal shear zones or sinking of the pluton as a deeper source reservoir was drained (Brown and Solar, 1998; Cruden, 1998; Wiebe and Collins, 1998).

Assuming relatively straightforward three-dimensional shapes for the pluton, subsidence of the floor or sinking of the Sausfjellet pluton would be expected to produce pluton-side-down shear zones in the aureole of the intrusion. However, shearing in the aureole of the pluton is predominantly pluton side up and/or strike-slip. In fact, floor subsidence is not a necessity for sub-

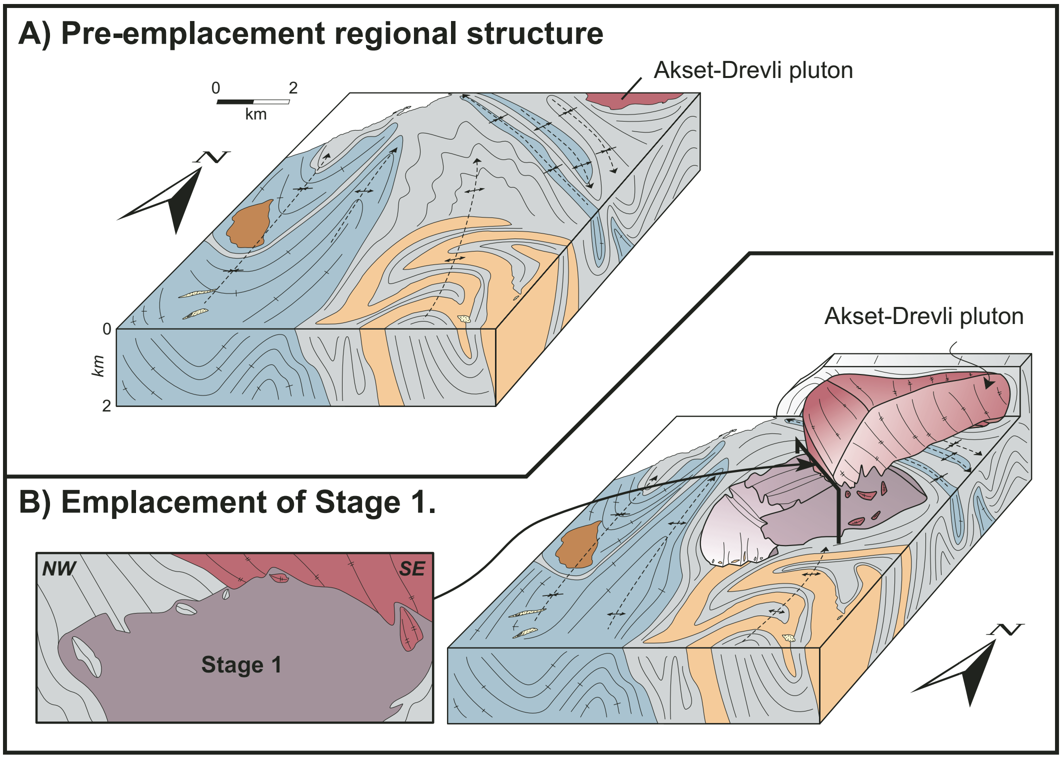

Figure 9. (A–D) Step-wise model with schematic cross sections for construction of the Sausfjellet pluton. Pre-emplacement structure from Dumond (2002). See text for explanation. (*Continued on following page*).

horizontal tabular construction of the Sausfjellet magma chamber if vertical displacement of the host rocks by stoping and lateral displacement by ductile flow are sufficient to make space for the pluton.

A Model for Construction and Deformation of the Sausfjellet Pluton

Figure 9 illustrates a possible geologic reconstruction of the study area prior to and during emplacement of the Sausfjellet pluton. The figure emphasizes the preexisting NNW-striking structural grain of the area (Fig. 9A; Dumond, 2002; Yoshinobu et al., 2002).

Emplacement of stage 1 magma was accommodated by stoping of the overlying Akset-Drevli pluton, marble, calc-silicate, and quartzo-feldspathic rocks (Fig. 9B). Akset-Drevli–type xenoliths occur within stage 1 and the moderately north-dipping southern contact of the Akset-Drevli pluton projects over the Sausfjellet pluton (Fig. 4A). Stoping was accompanied by lateral and downward ductile flow of the host rocks as indicated by the pluton-up, host-rocks–down kinematic relationships. Lateral and vertical translation of material around the growing magma chamber by ductile flow, boudinage, and displacement on marginal shear zones, coupled with downward transfer of xenoliths through the feeder conduit would account for the volume loss that is required at deeper levels.

Stage 2 magma was emplaced adjacent to or above stage 1 (Fig. 9C) and involved stoping of partially molten pelitic migmatitic host rocks along the western margin and projected roof. Continued growth of stage 2 resulted in deflection of the migmatitic pelitic gneiss due to lateral expansion of the chamber (Fig. 9C).

We propose that foundering of the central zone of stage 2 due to tilting of the crystal-mush pile and contemporaneous regional deformation (e.g., Table 1) resulted in coeval injection of the western/annular zone magma (see schematic cross sections in Fig. 9C). During and after emplacement of the western/annular zone, translation of the crystal-mush pile toward the southwest continued, which resulted in deformation of the igneous layering as indicated by the predominant southwest-plunging lineation and top-to-the-southwest normal sense of shear in the pluton (Fig. 3).

Because the axis of the synformal magmatic foliation trajectory pattern and magmatic foliations cross lithologic and geochemical boundaries, the final fabric pattern must have been produced after the magma chamber was already constructed. We suggest that igneous layering and structures associated with southwest-directed foundering (e.g., lineations, magmatic shear bands) formed during the duration of chamber construction and represent processes operative during construction and petrologic evolution of the chamber. The southwest-directed shearing within the chamber may reflect compaction processes associated with expulsion and emplacement of the western annular zone. Magmatic foliations probably formed throughout the history of chamber formation; however, based on crosscutting relationships between the foliations, xenoliths, and compositional boundaries, we suggest that the final geometry of magmatic foliations may be the result of combined foundering of the magma chamber and regional northwest-southeast–directed contraction during final solidification of the pluton (e.g., Benn et al., 2001). We note, however, structures associated with a ca. 445 Ma contractional event have only been identified so far in the Sausfjellet pluton–host-rock system.

CONCLUSIONS

The Sausfjellet pluton (445 ± 11 Ma) was emplaced at a pressure of ~700 MPa (25–30 km) into marbles, calc-silicate, diorite, quartzo-feldspathic gneiss, and pelitic migmatite in at least two stages, one gabbroic and one dioritic. Emplacement was accommodated by simultaneous stoping and ductile flow of the host rocks that are divided into predominantly carbonate on the east and pelitic/migmatitic on the west. Pluton-bounding folds and shear zones define an ~1-km-wide structural aureole. The presence of carbonate, calc-silicate, dioritic, and in all stages of the intrusion implies that stoping occurred

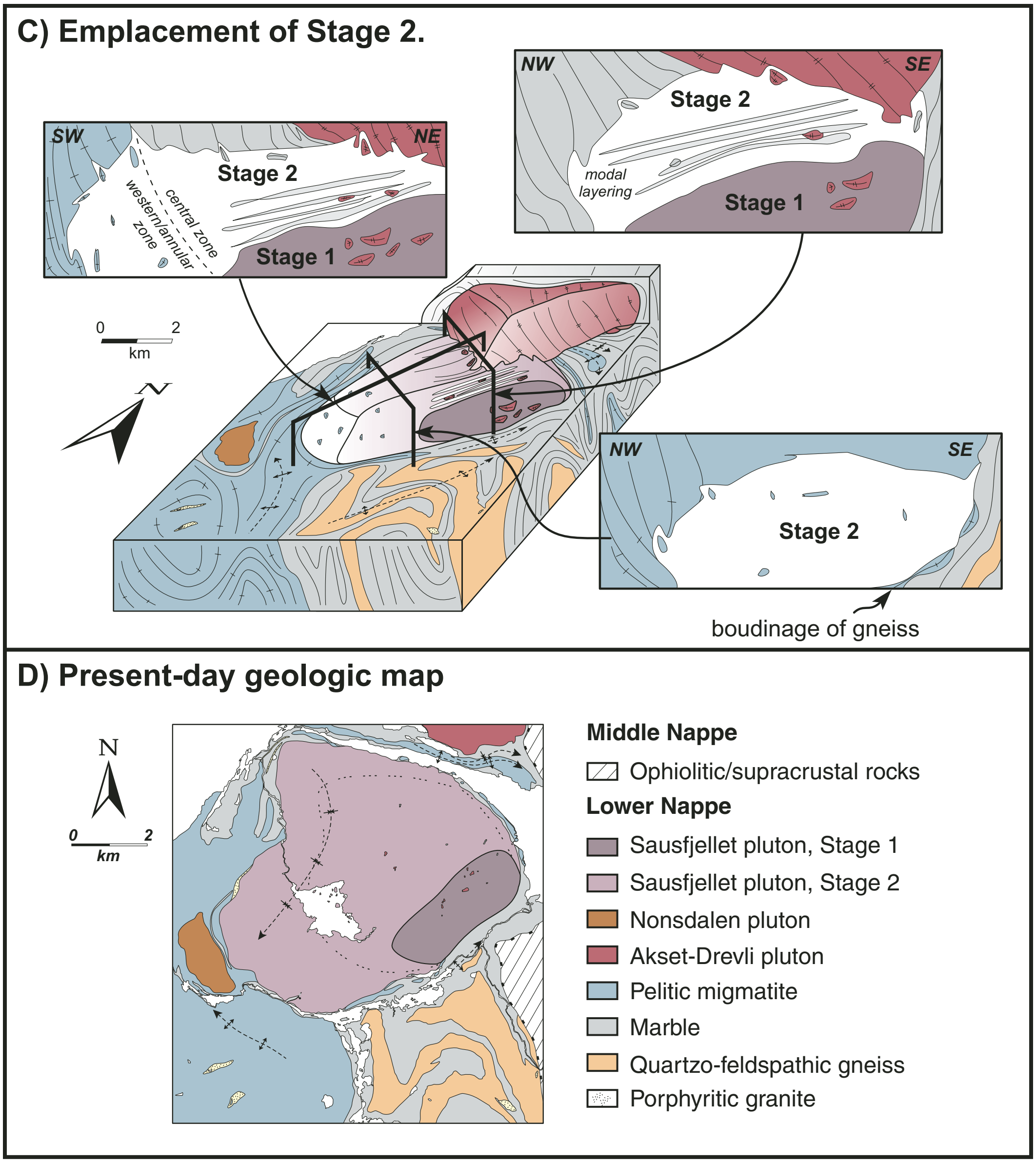

Figure 9 (*continued*).

throughout the emplacement history of the pluton. The lack of pelitic/migmatitic xenoliths is consistent with assimilation of partially molten pelitic gneiss. The aggrading, layered floor of cumulus minerals provided a rheologically strong medium that trapped the xenoliths as they were incorporated into the chamber.

The late-stage, shallowly southwest-plunging, synformal foliation trajectory pattern and mineral lineations in the pluton reflect, in part, foundering and deformation of a crystal cumulate pile toward the southwest after construction of the magma chamber. Regional ca. 445 Ma contraction may also have contributed to folding of the magma chamber, however structures of this age are confined to the pluton–host-rock systems. Combined with the companion petrological/geochemical study of Barnes et al. (2004), this study reveals the complex interplay of physical emplacement-related processes and the magmatic evolution of a magma chamber and suggests that stoping and xenolith assimilation may be important processes during magma evolution in the middle and lower crust.

ACKNOWLEDGMENTS

We thank Melanie Barnes, the Norwegian Geological Survey, Tore Prestvik, and Petra and Håkon Aune for outstanding logistical support. Our ideas regarding the research presented here have been greatly influenced by a number of thought-provoking conversations with Keegan Schmidt, Øystein Nordgulen, Tore Prestvik, Roar Sandøy, Scott Paterson, Geoff Pignotta, and Christopher L. Andronicos. We thank Associate Editor Rick Law, Keith Benn, and an anonymous reviewer for their comments and suggestions on the submitted manuscript. Funding to support this research was provided by National Science Foundation grant EAR-9814280 (Barnes), NSF grant EAR-0106557 (Yoshinobu), the Texas Tech University Research Enhancement Fund (Yoshinobu), and a Texas Tech University Mr. and Mrs. Carl H. Gelin Graduate Student Loan to G. Dumond.

REFERENCES CITED

Barnes, C.G., and Prestvik, T., 2000, Conditions of pluton emplacement and anatexis in the Caledonian Bindal Batholith, north-central Norway: Norwegian Journal of Geology, v. 80, p. 259–274.

Barnes, C.G., Prestvik, T., Nordgulen, Ø., and Barnes, M.A., 1992, Geology of three dioritic plutons in Velfjord, Nordland: Norges Geologiske Undersøkelse Bulletin, v. 423, p. 41–54.

Barnes, C.G., Yoshinobu, A.S., Prestvik, T., Nordgulen, Ø., Karlsson, H.R., and Sundvoll, B., 2002, Mafic magma intraplating: Anatexis and hybridization in arc crust,

Bindal Batholith, Norway: Journal of Petrology, v. 43, p. 2171–2190, doi: 10.1093/PETROLOGY/43.12.2171.
Barnes, C.G., Dumond, G., Yoshinobu, A.S., and Prestvik, T., 2004, Assimilation and crystal accumulation during construction of a mid-crustal magma chamber: The Sausfjellet pluton, north-central Norway: Lithos, v. 75, p. 389–412, doi: 10.1016/J.LITHOS.2004.04.036.
Benn, K., Paterson, S.R., Lund, S.P., Pignotta, G.S., and Kruse, S., 2001, Magmatic fabrics in batholiths as markers of regional strains and plate kinematics: Example of the Cretaceous Mt. Stuart batholith: Physics and Chemistry of The Earth, v. 26, p. 343–354, doi: 10.1016/S1464-1895(01)00064-3.
Brown, M., and Solar, G.S., 1998, Granite ascent and emplacement during contractional deformation in convergent orogens: Journal of Structural Geology, v. 20, p. 1365–1393, doi: 10.1016/S0191-8141(98)00074-1.
Buddington, A.F., 1959, Granite emplacement with special reference to North America: Geological Society of America Bulletin, v. 70, p. 671–748.
Clarke, D.B., Henry, A.S., and White, M.A., 1998, Exploding xenoliths and the absence of "elephants' graveyards" in granite batholiths: Journal of Structural Geology, v. 20, no. 9–10, p. 1325–1343.
Clemens, J.D., and Mawer, C.K., 1992, Granitic magma transport by fracture propagation: Tectonophysics, v. 204, p. 339–360, doi: 10.1016/0040-1951(92)90316-X.
Cruden, A.R., 1998, On the emplacement of tabular granites: Journal of the Geological Society of London, v. 155, p. 853–862.
Daly, R.A., 1903, The mechanics of igneous intrusion: American Journal of Science, v. 16, p. 107–126.
Dumond, G., 2002, Magma chamber construction in the middle crust: Insights from the Sausfjellet pluton, Bindal Batholith, Norway [M.S. thesis]: Lubbock, Texas Tech University, 89 p.
Dumond, G., Yoshinobu, A.S., and Barnes, C.G., 2002, Strain patterns, stoping, and subsidence in the 7kb Sausfjellet pluton, central Norway: Geological Society of America Abstracts with Programs, v. 34, no. 5, p. A31.
Gustavson, M., 1981, Mosjøen-M: Norges Geologiske Undersøkelse Map, scale 1:250,000.
Hogan, J.P., and Gilbert, M.C., 1995, The A-type Mount Scott Granite sheet: Importance of crustal magma traps: Journal of Geophysical Research, v. 100, p. 15,779–15,792, doi: 10.1029/94JB03258.
Holder, M.T., 1979, An emplacement mechanism for post-tectonic granites and its implications for their geochemical features, *in* Atherton, M.P., and Tarney, J., Origin of granite batholiths: Geochemical evidence: Kent, UK, Shiva, p. 116–128.
Hutton, D.W.H., 1988, Granite emplacement mechanisms and tectonic controls: Inferences from deformation studies: Transactions of the Royal Society of Edinburgh, v. 79, p. 245–255.
Irvine, T.N., 1980, Magmatic infiltration metasomatism, double-diffusive fractional crystallization, and adcumulus growth in the Muskox Intrusion and other layered intrusions, *in* Hargraves, R.B., ed., Physics of Magmatic Processes: Princeton, Princeton University Press, p. 325–383.
Kollung, S., and Myrland, R., 1970, Velfjord: Norges Geologiske Undersøkelse Map I 18, scale 1:100,000.
Marsh, B.D., 1982, On the mechanics of igneous diapirism, stoping, and zone melting: American Journal of Science, v. 282, p. 808–855.
McBirney, A.R., 1996, The Skaergaard Intrusion, *in* Cawthorn, R.G., ed., Layered Intrusions, Developments in Petrology 15: Amsterdam, Elsevier, p. 147–177.
McNulty, B.A., Tobisch, O.T., Cruden, A.R., and Gilder, S., 2000, Multistage emplacement of the Mount Givens Pluton, central Sierra Nevada Batholith, California: Geological Society of America Bulletin, v. 112, p. 119–135.
Miller, R.B., and Paterson, S.R., 1999, In defense of magmatic diapirs: Journal of Structural Geology, v. 21, p. 1161–1173, doi: 10.1016/S0191-8141(99)00033-4.
Morgan, S.S., Law, R.D., and Nyman, M.W., 1998, Laccolith-like emplacement model for the Papoose Flat pluton based on porphyroblast-matrix analysis: Geological Society of America Bulletin, v. 110, p. 96–110, doi: 10.1130/0016-7606(1998)1102.3.CO;2.
Nordgulen, Ø., and Sundvoll, B., 1992, Strontium isotope composition of the Bindal Batholith, Central Norwegian Caledonides: Norges Geologiske Undersøkelse Bulletin, v. 423, p. 19–39.
Nordgulen, Ø., Bickford, M.E., Nissen, A.L., and Wortman, G.L., 1993, U-Pb zircon ages from the Bindal Batholith, and the tectonic history of the Helgeland Nappe Complex, Scandinavian Caledonides: Journal of the Geological Society of London, v. 150, p. 771–783.
Paterson, S.R., and Miller, R.B., 1998, Magma emplacement during arc-perpendicular shortening: An example from the Cascades crystalline core, Washington: Tectonics, v. 17, p. 571–586, doi: 10.1029/98TC01604.
Paterson, S.R., Fowler, T.K., Jr., and Miller, R.B., 1996, Pluton emplacement in arcs: A crustal-scale exchange process: Transactions of the Royal Society of Edinburgh: Earth Sciences, v. 87, p. 115–123.
Patiño Douce, A.E., and Johnston, A.D., 1991, Phase equilibria and melt productivity in the pelitic system: Implications for the origin of peraluminous granitoids and aluminous granulites: Contributions to Mineralogy and Petrology, v. 107, p. 202–218.
Petford, N., 1996, Dykes or diapers?: Transactions of the Royal Society of Edinburgh: Earth Sciences, v. 87, p. 105–114.
Pitcher, W.S., 1979, The nature, ascent, and emplacement of granite magmas: Journal of the Geological Society of London, v. 139, p. 627–662.
Rubin, A.M., 1993, Dikes vs. diapirs in visco-elastic rock: Earth and Planetary Science Letters, v. 117, p. 653–670, doi: 10.1016/0012-821X(93)90109-M.
Skaarup, P., Prestvik, T., Kollung, S., and Myrland, R., 1974, Bindal: Norges Geologiske Undersøkelse Map I 19, scale 1:100,000.
Skjerlie, K.P., Patiño Douce, A.E., and Johnston, A.D., 1993, Fluid absent melting of a layered crustal protolith: Implications for the generation of anatectic granites: Contributions to Mineralogy and Petrology, v. 114, p. 365–378.
Thorsnes, T., 1985, The tectonostratigraphical development of the Nordfjellmark area, S. Nordland [Ph.D. thesis]: Bergen, University of Bergen, 228 p.
Thorsnes, T., and Løseth, H., 1991, Tectonostratigraphy in the Velfjord-Tosen region, southwestern part of the Helgeland Nappe Complex, Central Norwegian Caledonides: Norges Geologiske Undersøkelse Bulletin, v. 421, p. 1–18.
Tikoff, B., and Teyssier, C., 1992, Crustal-scale en echelon "P-shear" tensional bridges: A possible solution to the batholithic room problem: Geology, v. 20, p. 927–930, doi: 10.1130/0091-7613(1992)0202.3.CO;2.
Tikoff, B., St. Blanquat, M., and Teyssier, C., 1999, Translation and the resolution of the pluton space problem: Journal of Structural Geology, v. 21, p. 1109–1117, doi: 10.1016/S0191-8141(99)00058-9.
Vigneresse, J.L., 1995, Control of granite emplacement by regional deformation: Tectonophysics, v. 249, p. 173–186, doi: 10.1016/0040-1951(95)00004-7.
Wiebe, R.A., and Collins, W.J., 1998, Depositional features and stratigraphic sections in granitic plutons: Implications for the emplacement and crystallization of granitic magma: Journal of Structural Geology, v. 20, p. 1273–1289, doi: 10.1016/S0191-8141(98)00059-5.
Yoshinobu, A.S., Barnes, C.G., Nordgulen, Ø., Prestvik, T., Fanning, M., and Pedersen, R.-B., 2002, Ordovician magmatism, deformation, and exhumation in the Caledonides of central Norway: An orphan of the Taconic orogeny?: Geology, v. 30, p. 883–886, doi: 10.1130/0091-7613(2002)0302.0.CO;2.
Yoshinobu, A.S., Fowler, T.K., Paterson, S.R., Llambias, E., Sato, A., and Tickji, H., 2003, A view from the roof: Magmatic stoping in the shallow crust, Chita pluton, Argentina: Journal of Structural Geology, v. 25, p. 1037–1048, doi: 10.1016/S0191-8141(02)00149-9.

Manuscript Received by the Society 4 August 2003
Revised Manuscript Received 23 August 2004
Manuscript Accepted 3 September 2004

Printed in the USA